Spatially resolved characterization of chemical species and crystal structures in $CuInS_2$ and $CuGa_xSe_y$ thin films using Raman microscopy

Thomas Schmid[*,1], Christian Camus[2], Sebastian Lehmann[2], Daniel Abou-Ras[2], Christian-Herbert Fischer[2,3], Martha Christina Lux-Steiner[2], and Renato Zenobi[1]

[1] Department of Chemistry and Applied Biosciences, ETH Zurich, 8093 Zurich, Switzerland
[2] Helmholtz Centre Berlin for Materials and Energy, Glienicker Str. 100, 14109 Berlin, Germany
[3] second affiliation: Free University Berlin, Institute of Chemistry, Fabeckstr. 34-36, 14195 Berlin, Germany

Received zzz, revised zzz, accepted zzz
Published online zzz (Dates will be provided by the publisher.)

PACS 61.66.Fn, 78.30.Hv, 68.37.Ps, 68.37.Lp

* Corresponding author: e-mail schmid@org.chem.ethz.ch, Phone: +41 44 6326112, Fax: +41 44 6321292

This study demonstrates the potential of Raman microscopy in the analysis of thin film cross-sections. Raman maps of the photovoltaic material $CuInS_2$ (CIS), which was prepared by the spray ion layer gas reaction method, revealed the spatial distribution of two different CIS modifications – chalcopyrite-type and CuAu I-type CIS – as well as contaminants and segregates with a lateral resolution of ca. 400 nm. Additionally, the chemical heterogeneity of a $CuGaSe_2/CuGa_3Se_5$ bilayer stack was clearly resolved. Raman microscopy provides a convenient way to simultaneously probe the chemical and structural properties of a sample. Based on Raman spectra, chemical species and even different crystal structures of inorganic compounds can be identified. Knowledge of the distribution of different phases and contaminants in thin films is crucial for further improvements of the coating process.

1 Introduction Wide band-gap copper-containing chalcopyrites, such as $CuInS_2$ (CIS) and $CuGaSe_2$ have attracted considerable interest as absorber materials in thin-film solar cells [1]. $CuInS_2$ exhibits an optical band gap (1.5 eV) ideally matching the solar spectrum, whilst $CuGaSe_2$ is a candidate for the top cell in tandem solar cells [1]. The efficiency of such solar cells is greatly dependent on the composition as well as on crystal structure and purity of the compounds involved [2].

In this study, cross-sections of thin film solar cell absorbers based on polycrystalline CIS have been characterized, which were prepared by the spray ion layer gas reaction (ILGAR) method on molybdenum-coated glass substrates [3]. These films were found to consist of two regions of different morphology (Figure 1). In the lower part of the film, a stack of approx. 30-nm thick CIS layers is found. By transmission electron microscopy (TEM) and Raman spectroscopy it was shown that these CIS layers are separated by interlayers containing elemental carbon. On top of this part, a well-crystallized region with grain sizes of up to several hundred nanometers is located. Additionally, a thin (about 20 nm) MoS_2 layer formed at the molybdenum/CIS-interface, and segregated copper sulfide species on the film surface can be observed [4].

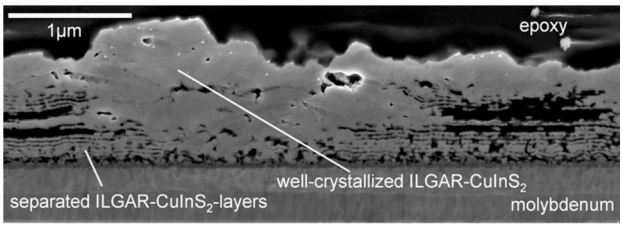

Figure 1 Scanning electron microscopy (SEM) image of an ILGAR CIS sample showing well-crystallized and layered CIS on a Molybdenum-coated glass substrate.

The fine structure of this ILGAR CIS film makes chemical and structural characterization a challenge. Cross-sectional TEM samples of ILGAR CIS were analyzed by Raman microscopy. In contrast to the usually

used 'point spectroscopy', which only probes the investigated samples locally on a few selected spots, Raman mapping was performed here by scanning the sample and collecting the whole spectrum at every pixel. The results demonstrate the potential of Raman microscopy in this field of application. Based on Raman spectra, not only different chemical species, but even different crystal structures of the same compound can be distinguished. Since the presence of secondary phases of the absorber material CIS is known to be detrimental for the solar cell efficiency, a mapping of the distribution of different crystal structures is highly desirable [2].

2 Experimental

2.1 Apparatus For Raman microscopy, an upright NTEGRA Spectra system from NT-MDT (Zelenograd/Moscow, Russia) was employed. The system is equipped with an upright confocal laser microscope, an atomic force microscope (AFM), a white-light video microscope for rough observation/alignment of the sample, a photomultiplier tube (PMT) detector for confocal imaging, and a Raman spectrograph equipped with a charge-coupled device (CCD). It allows simultaneous AFM and optical measurements on exactly the same part of transparent and opaque samples. All optical measurements were performed using a 100× long working-distance objective with a numerical aperture (NA) of 0.7 for both, excitation and collection of the backscattered light from the sample. A HeNe laser was used for excitation (λ = 632.8 nm, ca. 5 mW at the sample, corresponding to an irradiance on the order of 10^6 W/cm^2). The measurements are controlled by NT-MDT's Nova software. A rough alignment of the sample can be performed using micrometer screws and white-light microscope observation. Subsequently, software-controlled mapping experiments were carried out by scanning the sample (maximum scan range ca. 100 µm × 100 µm).

2.2 Samples The polycrystalline CIS thin films that are described in this paper have been prepared by the spray ILGAR method on molybdenum-coated glass substrates [3]. A $CuGaSe_2/CuGa_3Se_5$ bilayer stack sample was prepared by chemical close-spaced vapor transport (CCSVT) [5]. All samples were prepared by the face-to-face method [6] in the form of standard TEM samples, so that two thin films could be investigated at the same time. The samples were mechanically ground to a thickness of about 30 µm and thinned to a thickness of 100–200 nm by ion etching (Ar^+ ions, 4 kV, 0.5 mA) under an angle of 11–13°.

3 Results and discussion

3.1 CIS sample Raman spectra of a Spray ILGAR CIS thin film cross-section were collected with a 12 s integration time per pixel. Figure 2 shows typical Raman spectra that were collected on different parts of the sample. They represent mixtures of different components, but the spectra selected here are dominated by one chemical/crystalline species, such as CH CIS (Trace (1)), CA/disordered CIS (Trace (2)), and Cu_xS_y (Trace (3)).

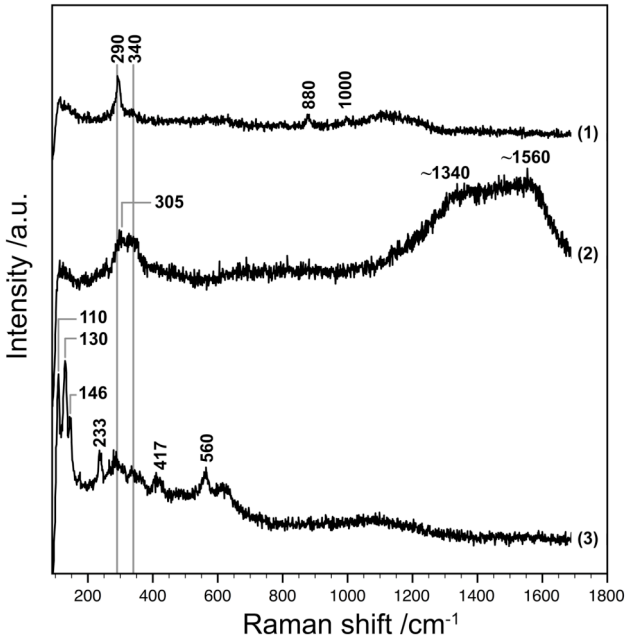

Figure 2 Typical Raman spectra collected on different parts of a CIS TEM sample. The three spectra are dominated by bands of CH CIS (1), CA/disordered CIS (2), and Cu_xS_y (3).

The most prominent CIS bands are found in the range of ca. 270–370 cm^{-1}. The most prominent modes of the two modifications of CIS – chalcopyrite-type (CH) CIS and CuAu I-type (CA) CIS – are the A_1 modes of both phases at 290 cm^{-1} (Trace (1)) and 305 cm^{-1} (Trace (2)), respectively [7]. However, it was observed that in Spray ILGAR CIS films, the disorder induced in the films by the presence of CA CIS is accompanied by an increased intensity of the $B_2{}^1{}_{LO}$ and $E^1{}_{LO}$ modes of CH CIS at about 340 cm^{-1} [4]. Therefore, the intensity of the band located at about 340 cm^{-1} can be regarded as a measure for the degree of disorder and for the amount of CA CIS present in the films. Spectral interferences with $CuIn_5S_8$ and In_2O_3, which also might be present in the sample, can be ruled out due to their Raman intensities. In contrast to the 1:1-intensity ratio of the 305-cm^{-1} and 340-cm^{-1} modes in the spectrum of CA CIS observed here, the bands of $CuIn_5S_8$ in the same range have a ratio of 7:1 [4]. The detection of In_2O_3 can be ruled out due to the 20–80× lower intensity of its most prominent band at 306 cm^{-1} compared to the A_1 modes of the two CIS modifications [4]. Two broad, overlapping bands at ca. 1340 cm^{-1} and 1560 cm^{-1}, which correspond to the D and G modes of nanocrystalline or amorphous carbon phases [8], were also observed in the spectra showing strong association with CA CIS (Trace (2)). This is in agreement with the findings of TEM/EDX, which reveal that in the lower part of the absorbers nanometer-thin layers containing the elements Cu, In, and S are separated by carbon-rich layers [4]. Spectrum (3) in Figure (1) is

dominated by bands that can be assigned to Cu_xS_y. The segregation of binary copper phases on the film surface has been frequently observed in Cu chalcopyrite films [9]. For exact determination of the Cu:S ratio, reference measurements with different well-characterized copper sulfides would be necessary. For example, the band at 417 cm^{-1} is described in the literature to be characteristic for Cu_xS_y species with x<y, whereas the 146-cm^{-1} band is known to be present in the spectra of copper sulfides with Cu:S ratios of 1:1 to 1.4:1 [10].

For a spatially resolved chemical analysis, the sample was scanned over a range of 10 µm × 10 µm, and a Raman map with 80 × 80 pixels was collected within ca. 21 h. Figure 3 shows distributions of different species over the sample area, which are based on the integrated intensity of the following ranges in the Raman spectra: 133–156 cm^{-1}, Cu_xS_y; 260–380 cm^{-1}, total CIS; 220–300 cm^{-1}, CH CIS; 300–380 cm^{-1}, CA/disordered CIS; 1100–1700 cm^{-1}, carbon. The first and last 10 cm^{-1} of every measurement range were used to calculate a linear baseline, which was subtracted before calculating the integral of the Raman bands. In the case of the sharp Cu_xS_y band at 146 cm^{-1}, only 1 cm^{-1} on both ends of the measurement range was used for baseline calculation. The spatial resolution was estimated based on the full width at half maximum (FWHM) of the smallest structures in Figure 3 (c) to be 375 nm ± 125 nm (3 ± 1 pixels). The lateral resolution of ca. 400 nm is in good agreement with the apparent size of nanoparticles much smaller than the laser focus (data not shown).

The Raman map of CIS in Figure 3 (b) reveals a layered structure of CIS with the dark areas in the middle (e.g. visible on the left border of the image) representing the epoxy glue used in the face-to-face sample preparation method. Thus, the structure is in good agreement with the schematic representation in Figure 3 (a). Figure 3 (c) and (d) reveal that the CIS layers consist of two different modifications, i.e. CH CIS and CA CIS. CA CIS has almost the same distribution as amorphous/nanocrystalline carbon (Figure 3 (f)). This lets us assume that the stacked CIS layers in the lower part of the CIS sample found in TEM experiments contain large amounts of CA CIS separated by amorphous or nanocrystalline carbon layers. In agreement with the SEM image in Figure 1, there is a crystalline CIS layer with ca. 1-µm-thick crystals on top of the layered CIS (Figure 3 (c)). Raman microscopy clearly shows that the well-crystallized part consists of CH CIS, which is the desired phase for photovoltaic applications, whilst the formation of CA CIS in the ILGAR process might be the reason for the still low solar cell efficiency [2].

For the understanding of the growth process of the Spray ILGAR CIS films, the distributions of carbon and Cu_xS_y are of paramount interest. An example for the latter is shown in Figure 3 (e). Obviously, copper sulfide has formed on top of three CIS crystallites due to segregation during the ILGAR process.

These experiments demonstrate how Raman microscopy can reveal the distribution of the various phases in Spray ILGAR CIS thin films. Thereby, it provides useful information, which helps to understand the growth mechanism and thus provides a basis for further improvements of the process.

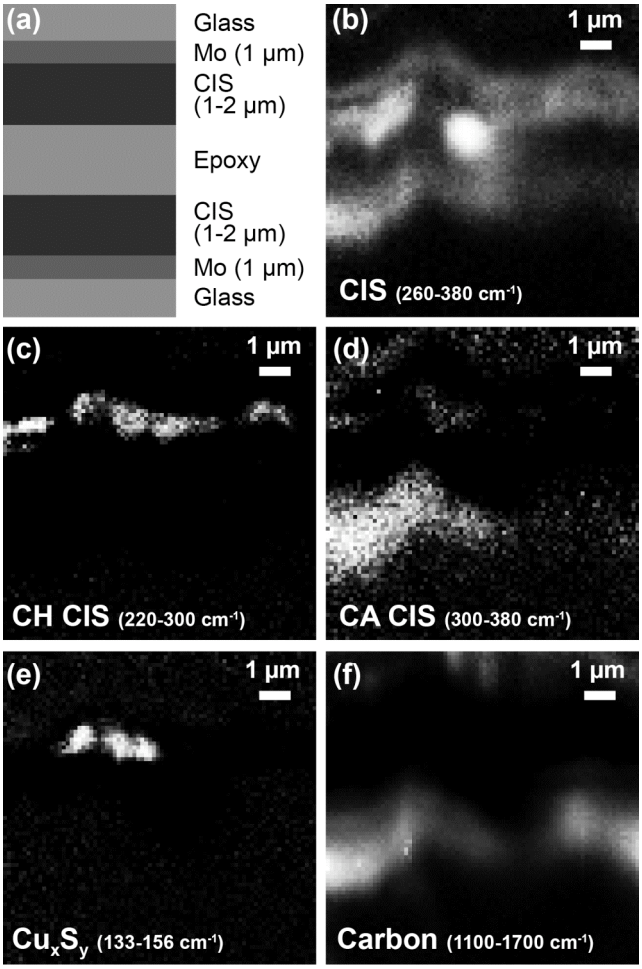

Figure 3 Schematic representation of the layered structure of a CIS cross-section (a) and Raman intensity maps collected on the same part of the sample corresponding to the following compounds: both CIS modifications (b), CH CIS (c), CA/disordered CIS (d), Cu_xS_y (e), and amorphous / nanocrystalline carbon (f).

3.2 $CuGaSe_2$/$CuGa_3Se_5$ sample Under the same conditions (632.8 nm, 5 mW at the sample), Raman mapping of a $CuGaSe_2$/$CuGa_3Se_5$ cross-section was performed. Figure 4 (a) shows an AFM topography image that was collected in semicontact mode. The image reveals crystals that are arranged in two layers (both from bottom left to top right of the image). AFM artifacts, such as horizontal lines at the edges of the crystals, are due to the relatively big height differences of up to 5.5 µm, which is close to the maximum z-scan range of the AFM used in this study.

A Raman map of the 10 × 6-$µm^2$ area was collected with a resolution of 20 × 12 pixels. The mapping was performed with the AFM in feedback, which controlled the movement of the sample in z direction, in order to reduce

topography artifacts in the Raman measurements. The most prominent bands in the Raman spectra were a sharp band at 184 cm^{-1} ($CuGaSe_2$) and two broad bands at 258 cm^{-1} and 960 cm^{-1} ($CuGa_3Se_5$), respectively. Integrals of Raman intensities were calculated after baseline correction as described above. In Figure 4 (b) and (c), the intensities of Raman bands assignable to $CuGa_3Se_5$ and $CuGaSe_2$, respectively, are mapped out. The Raman maps clearly reveal the two-layered structure of the sample as schematically shown for comparable samples in Ref. [5].

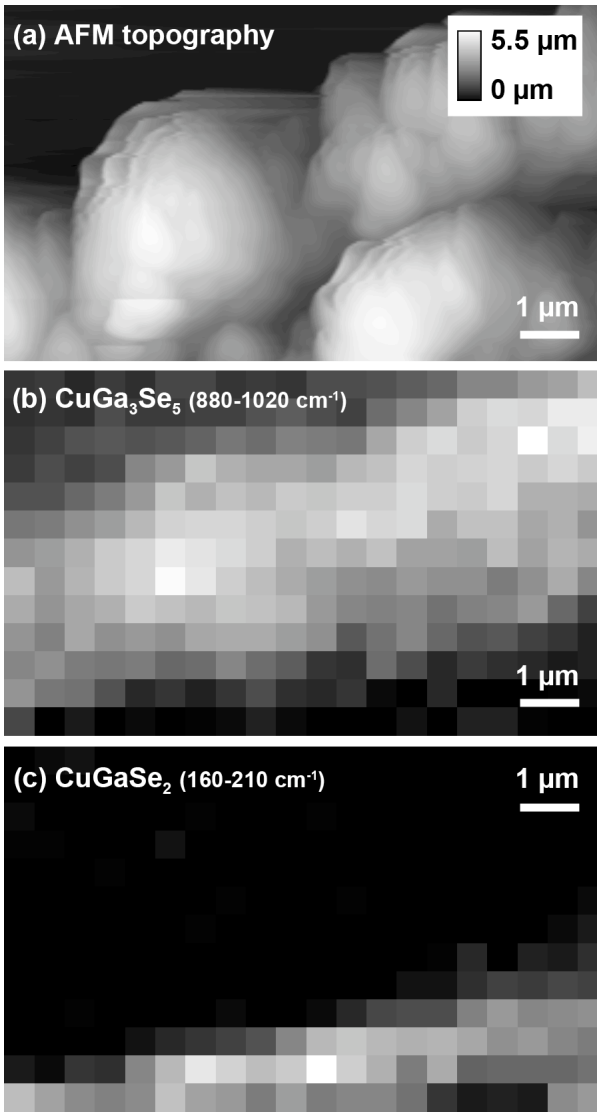

Figure 4 AFM topography (a) and Raman maps (b, c) of the two components of a $CuGaSe_2/CuGa_3Se_5$ system.

4 Conclusion This study clearly demonstrates the potential of Raman microscopy for investigation of cross-sections of inorganic samples, such as chalcopyrite thin-film solar cell absorber layers. Raman microscopy provides a convenient way to simultaneously probe the chemical and structural properties of an extended sample area. Not only different chemical species, but also different crystal structures of the same compound can be distinguished, and their spatial distribution can be mapped out with a resolution of ca. 400 nm. Raman mapping of polished cross-sections of ILGAR CIS samples will be the subject of a further study. First measurements with a 532-nm laser have revealed that spectra with a similar signal-to-noise ratio as shown here can be obtained within 0.1–1 s due to the λ^{-4}-dependence of the Raman scattering intensity, which will reduce the measurement time for a mapping from ca. 21 h to 10 min–1 h. Also, tip-enhanced Raman spectroscopy (TERS) with the described setup is under development, which can provide a spatial resolution of 10–50 nm [11].

Acknowledgements The authors acknowledge the Swiss National Science Foundation (R'EQUIP project number 206021-117373) for financial support.

References

[1] S. Siebentritt, Thin Solid Films **403-404**, 1 (2002).
[2] J. Álvarez-García, E. Rudigier, N. Rega, B. Barcones, R. Scheer, A. Perez-Rodriguez, A. Romano-Rodriguez and J. R. Morante, Thin Solid Films **431**, 122 (2003).
[3] C. Camus, N. A. Allsop, S. E. Gledhill, W. Bohne, J. Röhrich, I. Lauermann, M. C. Lux-Steiner and Ch.-H. Fischer, Thin Solid Films **516**, 7026 (2008).
[4] C. Camus, PhD thesis, Freie Universität Berlin (2008). http://www.diss.fu-berlin.de/diss/receive/FUDISS_thesis_000000006014.
[5] S. Lehmann, M. Bär, D. Fuertes Marrón, P. Pistor, S. Wiesner, M. Rusu, I. Kötschau, I. Lauermann, A. Grimm, S. Sokoll, C.-H. Fischer, T. Schedel-Niedrig, M.C. Lux-Steiner and Ch. Jung, Thin Solid Films **511-512**, 623 (2006).
[6] J. C. Bravman and R. Sinclair, J. Electron Microsc. **1**, 53 (1984).
[7] J. Álvarez-García, A. Perez-Rodriguez, B. Barcones, A. Romano-Rodriguez, J. R. Morante, A. Janotti, S. H. Wei, and R. Scheer, Appl. Phys. Lett. **80**, 562 (2002).
[8] A. Ferrari and J. Robertson, Phys. Rev. B **61**, 14095 (2000).
[9] R. Klenk, T. Walter, H.-W. Schock, D. Cahen, Adv. Mater. **5** 114 (1993).
[10] C. G. Munce, G. K. Parker, S. A. Holt, G. A. Hoppe, Colloid Surface A **295**, 152 (2007).
[11] T. Schmid, B.S. Yeo, W. Zhang and R. Zenobi, in: Tip Enhancement, edited by S. Kawata and V. Shalaev (Elsevier, 2007), p. 115.